16th European Signal Processing Conference (EUSIPCO 2008), Lausanne, Switzerland, August 25-29, 2008, copyright by EURASIP

SOFT SPHERE DECODER FOR AN ITERATIVE RECEIVER IN TIME-VARYING MIMO CHANNELS

Charlotte Dumard[1], *Joakim Jaldén*[2] *and Thomas Zemen*[1]

[1] ftw. Forschungszentrum Telekommunikation Wien, Donau City Str. 1/3, A-1220 Vienna, Austria
{dumard, zemen}@ftw.at

[2] Vienna University of Technology, Guhausstr. 25-29 // 389, A-1040 Vienna, Austria
joakim.jalden@nt.tuwien.ac.at

ABSTRACT

Iterative multi-user detection based on linear minimum mean square error (LMMSE) filtering in time-variant MIMO systems involves high computational complexity. Sphere decoding after an initial interference cancelation step allows for substantial complexity reduction if the sphere decoder exploits the reduced rank time-variant channel subspace. However, a performance loss in terms of bit error rate (BER) versus signal to noise ratio (SNR) is incurred mainly due to the hard decision supplied by the sphere decoder. Building on past work of the authors we demonstrate in this paper that a soft output max-log sphere decoder can exploit the reduced rank time-variant channel subspace as well. We show that the proposed sphere decoder solution provides a computationally more efficient approach, with maintained quality in terms of bit error rate compared to an iterative LMMSE multi-user detector.

1. INTRODUCTION

We focus on the uplink of a MC-CDMA system based on orthogonal frequency division multiplexing (OFDM). The users move at vehicular speed, hence the MIMO channel from each user to the base-station is time-varying. The receiver at the base-station performs iterative multi-user (MU) detection using parallel interference cancelation (PIC) followed by a sphere decoder implemented on a per user basis. In [1], hard outputs of the sphere decoder are used. This method has been shown to be less complex than a linear minimum mean square error filter that would detect all users jointly. However, the hard sphere decoder, assuming perfect PIC, does not take residual interference into account and induces a substantial performance loss.

In this paper we replace the hard sphere decoder by a soft sphere decoder. The computation of log-likelihood ratios (LLR) lead to an increase of the complexity compared to hard sphere decoding. Still, the complexity remains about one order of magnitude below the linear minimum mean square error (LMMSE) filter complexity.

Contribution of the paper: We develop a soft sphere decoder, using the complexity efficient subspace based implementation of a sphere decoder developed in [1] in order to compute the LLR, based on a method presented in [2]. The soft sphere decoder complexity is one order of magnitude higher than for hard sphere decoding and one order of magnitude lower than for LMMSE. The use of soft outputs allows reaching LMMSE performance.

Notation: We denote a column vector with elements a_i by $\boldsymbol{a}$. The transpose of a matrix $\boldsymbol{A}$ is given by $\boldsymbol{A}^{\mathrm{T}}$ and its conjugate transpose by $\boldsymbol{A}^{\mathrm{H}}$. A diagonal matrix with elements a_i is written as $\mathrm{diag}(\boldsymbol{a})$ and the $Q \times Q$ identity matrix as $\boldsymbol{I}_Q$. The norm of $\boldsymbol{a}$ is denoted $\|\boldsymbol{a}\|$.

This work has been founded by the EU project MASCOT.

Organization of the Paper: We describe the system model and iterative receiver with parallel interference cancelation in Sec. 2. The soft sphere decoder is presented in Sec. 3. Simulations results are shown in Sec. 4. Comments on the computational complexity are given in Sec. 5 and conclusions are drawn afterwards.

2. SYSTEM MODEL

In [1] we present a complexity efficient implementation of the sphere decoder in an iterative MU-MIMO receiver for a MC-CDMA uplink, based on the structure of the time-varying channel model. This paper builds on [1], using its implementation of a sphere decoder to compute the LLR with lower complexity.

2.1 Multi-Antenna Transmitter

Let us consider the transmitter of user $k \in \{1, \ldots, K\}$. We denote its transmit antenna $t \in \{1, \ldots, T\}$ by (k, t). $(M - J)T$ data symbols are jointly coded, interleaved, mapped to a QPSK constellation and split into T blocks of length $M - J$. Transmit antenna (k, t) sends a block of M OFDM symbols, including J distributed pilot symbols allowing for channel estimation. Data symbol $b_{(k,t)}[m]$ is spread over all N subcarriers using a spreading sequence $\boldsymbol{s}_{(k,t)} \in \mathbb{C}^N$ with i.i.d. elements from a QPSK constellation. Thus, transmit antenna (k, t) sends the OFDM symbols $\boldsymbol{s}_{(k,t)} b_{(k,t)}[m]$ for $m \notin \mathcal{P}$, where $\mathcal{P}$ is the set of pilot positions in each data block [3].

2.2 Time-Varying Channel Model

The iterative receiver structure is shown in Fig. 1. The receiver is equipped with R antennas. The propagation channel from transmit antenna (k, t) to receive antenna r is characterized by the frequency response $\boldsymbol{g}_{r,(k,t)}[m] \in \mathbb{C}^N$ at time instant m with elements $g_{r,(k,t)}[m, q]$. The index $q \in \{0, \ldots, N-1\}$ denotes the subcarrier index. The related effective spreading sequence is defined by

$$\tilde{\boldsymbol{s}}_{r,(k,t)}[m] = \mathrm{diag}(\boldsymbol{s}_{(k,t)}) \boldsymbol{g}_{r,(k,t)}[m] \,. \tag{1}$$

The maximum variation in time of the wireless channel is upper bounded by the maximum normalized one-sided Doppler bandwidth $\nu_{\mathrm{Dmax}} = \frac{v_{\max} f_{\mathrm{C}}}{c_0} T_{\mathrm{S}}$, where $v_{\max}$ is the maximum (supported) velocity, T_{S} is the OFDM symbol duration, f_{C} is the carrier frequency and c_0 the speed of light. Time-limited snapshots of the bandlimited fading process span a subspace with very small dimensionality. The same subspace is spanned by discrete prolate spheroidal (DPS) sequences [3] $\{u_i[m]\}$ defined as in [4].

We are interested in describing the time-varying frequency selective channel $\boldsymbol{g}_{r,(k,t)} \in \mathbb{C}^N$ for the duration of

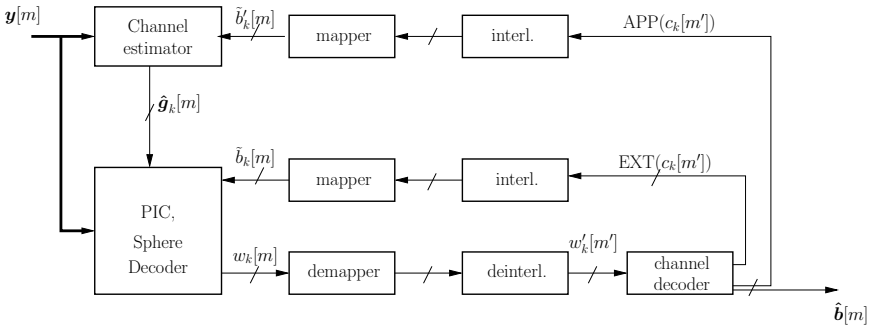

Figure 1: Iterative MC-CDMA receiver.

a single data block $\mathcal{I}_M = \{0, \ldots, M-1\}$. For $m \in \mathcal{I}_M$ we write $\boldsymbol{g}_{r,(k,t)}[m]$ as linear superposition of the first D DPS sequences, index limited to the time interval $\mathcal{I}_M$,

$$\tilde{\boldsymbol{g}}_{r,(k,t)}[m] = \boldsymbol{\Gamma}_{r,(k,t)} \boldsymbol{f}[m]\,, \tag{2}$$

where $\boldsymbol{f}[m] = [u_0[m], \ldots, u_{D-1}[m]]^{\mathrm{T}} \in \mathbb{C}^{\,D}$ for $m \in \mathcal{I}_M$. In practical cases, D is of the order of 3 to 5 [3]. Dedicated pilot symbols together with feedback soft symbols are used to estimate the coefficients in $\boldsymbol{\Gamma}_{r,(k,t)} \in \mathbb{C}^{\,N \times D}$, see [3].

Inserting (2) in (1) and after summation of the signals from all transmit antennas of all users, we obtain the signal at antenna r

$$\boldsymbol{y}_r[m] = \sum_{k=1}^{K} \sum_{t=1}^{T} \mathrm{diag}(\boldsymbol{s}_{(k,t)}) \boldsymbol{\Gamma}_{r,(k,t)} \boldsymbol{f}[m] b_{(k,t)}[m] + \boldsymbol{n}_r[m]\,,$$

where $\boldsymbol{n}_r$ is additive white Gaussian noise (AWGN) with zero mean and variance $\sigma^2 \boldsymbol{I}_N$. Denoting by $\boldsymbol{y}[m] = [\boldsymbol{y}_1[m]^{\mathrm{T}}, \ldots, \boldsymbol{y}_R[m]^{\mathrm{T}}]^{\mathrm{T}}$ the stacked vector containing the R received signals, we can write

$$\boldsymbol{y}[m] = \boldsymbol{\Gamma} \boldsymbol{F}[m] \boldsymbol{b}[m] + \boldsymbol{n}[m]\,,$$

where $\boldsymbol{\Gamma} = [\boldsymbol{\Gamma}_1 \cdots \boldsymbol{\Gamma}_K]$ and

$$\boldsymbol{\Gamma}_k = \begin{bmatrix} \mathrm{diag}(\boldsymbol{s}_{(k,1)}) \boldsymbol{\Gamma}_{1,(k,1)} & \cdots & \mathrm{diag}(\boldsymbol{s}_{(k,T)}) \boldsymbol{\Gamma}_{1,(k,T)} \\ \vdots & \ddots & \vdots \\ \mathrm{diag}(\boldsymbol{s}_{(k,1)}) \boldsymbol{\Gamma}_{R,(k,1)} & \cdots & \mathrm{diag}(\boldsymbol{s}_{(k,T)}) \boldsymbol{\Gamma}_{R,(k,T)} \end{bmatrix}$$

are time-independent. The matrix

$$\boldsymbol{F}[m] = \begin{bmatrix} \boldsymbol{f}[m] & \boldsymbol{0} & \boldsymbol{0} \\ \boldsymbol{0} & \ddots & \boldsymbol{0} \\ \boldsymbol{0} & \boldsymbol{0} & \boldsymbol{f}[m] \end{bmatrix} \in \mathbb{R}^{\,DKT \times KT}\,,$$

contains the time-varying basis expansion, $\boldsymbol{b}[m] = [b_{(1,1)}[m], \ldots, b_{(K,T)}[m]]^{\mathrm{T}} \in \mathbb{C}^{\,KT}$ contains all KT transmitted symbols and $\boldsymbol{n}$ is AWGN with zero mean and variance $\sigma^2 \boldsymbol{I}_{NR}$.

The contribution of user k stemming from symbols $\boldsymbol{b}_k[m] = [b_{(k,1)}[m], \ldots, b_{(k,T)}[m]]^{\mathrm{T}}$ is defined as

$$\boldsymbol{y}_k[m] = \boldsymbol{\Gamma}_k \boldsymbol{F}_0[m] \boldsymbol{b}_k[m] + \boldsymbol{n}_k[m]\,,$$

where $\boldsymbol{n}_k[m]$ is AWGN with zero mean and variance $\sigma^2 \boldsymbol{I}_{NR}$ and $\boldsymbol{F}_0[m]$ contains the first DT rows and T columns of $\boldsymbol{F}[m]$.

2.3 Parallel Interference Cancelation

We perform PIC for user k by removing the contribution of users $k' \neq k$ using soft-symbol estimates [5]

$$\begin{aligned} \tilde{\boldsymbol{y}}_k[m] &= \boldsymbol{y}[m] - \sum_{k' \neq k} \boldsymbol{\Gamma}_{k'} \boldsymbol{F}_0[m] \tilde{\boldsymbol{b}}_{k'}[m] \\ &\approx \boldsymbol{\Gamma}_k \boldsymbol{F}_0[m] \tilde{\boldsymbol{b}}_k[m] + \boldsymbol{n}_k[m]\,. \end{aligned} \tag{3}$$

The soft symbols in $\tilde{\boldsymbol{b}}_{k'}$ are computed from the extrinsic probabilities supplied by the BCJR decoder [6], from the previous iteration of the receiver.

3. SOFT SPHERE DECODING

For simplification, we omit the user index k in the following. For computational complexity reasons, sphere decoding is performed on a per user basis. Admittedly, under the assumption that all channels are independent and uncorrelated, the grouping of transmit antennas based on their physical co-location is not a prerequisite and any partitioning would do. However, for intuitive reasons we prefer the user basis partitioning.

3.1 Conversion Imaginary to Real Space

So far all elements are complex valued. The transmitted symbols $\boldsymbol{b}$ stem from a QPSK symbol alphabet $\mathcal{A} \in \{\frac{\pm 1 \pm \imath}{\sqrt{2}}\}$. However, the soft sphere decoder requires computations of log-likelihood ratios, which is somewhat simpler to perform in the real domain.

In order to convert the signal model into the real domain, we define the subscripts (r) and (i) respectively denoting the real and imaginary part of a complex, vector or matrix. Furthermore, we scale the input vector such that we consider entries for $\hat{\boldsymbol{b}}$ in $\{\pm 1\}$ only. We denote (time index m is omitted in these definitions)

$$\hat{\boldsymbol{b}} = \sqrt{2} \begin{bmatrix} \boldsymbol{b}^{(r)} \\ \boldsymbol{b}^{(i)} \end{bmatrix}, \quad \hat{\boldsymbol{y}} = \begin{bmatrix} \tilde{\boldsymbol{y}}^{(r)} \\ \tilde{\boldsymbol{y}}^{(i)} \end{bmatrix}, \quad \hat{\boldsymbol{n}} = \begin{bmatrix} \boldsymbol{n}^{(r)} \\ \boldsymbol{n}^{(i)} \end{bmatrix},$$

$$\hat{\boldsymbol{\Gamma}} = \begin{bmatrix} \boldsymbol{\Gamma}^{(r)} & -\boldsymbol{\Gamma}^{(i)} \\ \boldsymbol{\Gamma}^{(i)} & \boldsymbol{\Gamma}^{(r)} \end{bmatrix} \quad \text{and} \quad \hat{\boldsymbol{F}} = \begin{bmatrix} \boldsymbol{F}_0 & \boldsymbol{0} \\ \boldsymbol{0} & \boldsymbol{F}_0 \end{bmatrix}.$$

Then the system model (3) can be rewritten as

$$\hat{\boldsymbol{y}}[m] = \frac{1}{\sqrt{2}} \hat{\boldsymbol{\Gamma}} \hat{\boldsymbol{F}}[m] \hat{\boldsymbol{b}}[m] + \hat{\boldsymbol{n}}[m]\,. \tag{4}$$

Using the channel model (4), the maximum likelihood equation writes

$$\hat{\boldsymbol{b}}_{\mathrm{ML}}[m] = \underset{\boldsymbol{b}}{\mathrm{argmin}} \, \| \hat{\boldsymbol{y}}[m] - \frac{1}{\sqrt{2}} \hat{\boldsymbol{\Gamma}} \hat{\boldsymbol{F}}[m] \hat{\boldsymbol{b}}[m] \|^2$$

which becomes after QR-decomposition of $\hat{\boldsymbol{\Gamma}} = \hat{\boldsymbol{Q}}_\Gamma \hat{\boldsymbol{R}}_\Gamma$

$$\hat{\boldsymbol{b}}_{\mathrm{ML}}[m] = \underset{\boldsymbol{b}}{\operatorname{argmin}} \left\| \hat{\boldsymbol{z}}[m] - \hat{\boldsymbol{R}}_\Gamma \hat{\boldsymbol{F}}[m] \hat{\boldsymbol{b}}[m] \right\|^2 , \qquad (5)$$

where $\hat{\boldsymbol{z}}[m] = \sqrt{2}\hat{\boldsymbol{Q}}_\Gamma^{\mathrm{T}} \hat{\boldsymbol{y}}[m]$, $\hat{\boldsymbol{Q}}_\Gamma$ is unitary and $\hat{\boldsymbol{R}}_\Gamma$ is square upper triangular.

In [1], we developed a suitable implementation to solve (5), taking the block structure of the basis expansion matrix $\boldsymbol{F}[m]$ into account. Although proven less complex than LMMSE, this method introduces a substantial loss in performance. This loss is partly due to the fact that the hard sphere decoder assumes perfect interference cancelation and thus does not take residual interference into account. An additional loss is due to the fact that the BCJR decoder receives hard inputs.

To solve this problem, it is necessary to compute soft symbols to feed the BCJR decoder. The authors in [2] present a method to compute the LLR using sphere decoding to reduce the complexity. We will recall the method in the following, and apply our subspace based implementation, that is more suitable for time-varying channels.

3.2 Definition of the Log-Likelihood Ratios

Let us denote by $\lambda_{\mathrm{PRIOR}}(b_t)$, $\lambda_{\mathrm{POST}}(b_t)$ and $\lambda_{\mathrm{EXT}}(b_t)$ the *a priori*, *a posteriori* and *extrinsic* probabilities of $b_t = \hat{b}(t)$, respectively. For each $t \in \{1, \ldots, 2T\}$, these are given by

$$\begin{aligned} \lambda_{\mathrm{PRIOR}}(b_t) &= \ln\left(\frac{p(b_t=+1)}{p(b_t=-1)}\right), \\ \lambda_{\mathrm{POST}}(b_t) &= \ln\left(\frac{p(b_t=+1|\hat{\boldsymbol{z}})}{p(b_t=-1|\hat{\boldsymbol{z}})}\right) \quad \text{and} \\ \lambda_{\mathrm{EXT}}(b_t) &= \lambda_{\mathrm{POST}}(b_t) - \lambda_{\mathrm{PRIOR}}(b_t). \end{aligned} \qquad (6)$$

3.3 Explicit Computation of Extrinsic Probabilities

Let $\mathbb{B}_t^+$ and $\mathbb{B}_t^-$ be the subsets of $\{-1,+1\}^{2T}$ such that $b_t = +1$ or $b_t = -1$, respectively. We have

$$\begin{aligned} p(b_t = \pm 1|\hat{\boldsymbol{z}}) &= \sum_{\hat{\boldsymbol{b}} \in \mathbb{B}_t^{\pm}} p(\hat{\boldsymbol{b}}|\hat{\boldsymbol{z}}) = \sum_{\hat{\boldsymbol{b}} \in \mathbb{B}_t^{\pm}} p(\hat{\boldsymbol{z}}|\hat{\boldsymbol{b}}) \cdot p(\hat{\boldsymbol{b}})/p(\hat{\boldsymbol{z}}) \\ &= p(b_t = \pm 1)/p(\hat{\boldsymbol{z}}) \sum_{\hat{\boldsymbol{b}} \in \mathbb{B}_t^{\pm}} p(\hat{\boldsymbol{z}}|\hat{\boldsymbol{b}}) \prod_{t' \neq t} p(b_{t'}) \end{aligned}$$

leading to

$$\lambda_{\mathrm{POST}}(b_t) = \lambda_{\mathrm{PRIOR}}(b_t) + \ln\left(\frac{\sum_{\hat{\boldsymbol{b}} \in \mathbb{B}_t^+} p(\hat{\boldsymbol{z}}|\hat{\boldsymbol{b}}) \cdot \prod_{t' \neq t} p(b_{t'})}{\sum_{\hat{\boldsymbol{b}} \in \mathbb{B}_t^-} p(\hat{\boldsymbol{z}}|\hat{\boldsymbol{b}}) \cdot \prod_{t' \neq t} p(b_{t'})}\right).$$

We also know

$$\begin{aligned} p(b_{t'} = \pm 1) &= \frac{\exp\left(\pm \lambda_{\mathrm{PRIOR}}(b_{t'})\right)}{1 + \exp(\pm \lambda_{\mathrm{PRIOR}}(b_{t'}))} \\ &= \underbrace{\frac{\exp\left(-\lambda_{\mathrm{PRIOR}}(b_{t'})/2\right)}{1 + \exp(-\lambda_{\mathrm{PRIOR}}(b_{t'}))}}_{A_{t'}} \cdot \exp\left(\pm \tfrac{\lambda_{\mathrm{PRIOR}}(b_{t'})}{2}\right) \\ &= A_{t'} \exp\left(b_{t'} \tfrac{\lambda_{\mathrm{PRIOR}}(b_{t'})}{2}\right). \end{aligned}$$

and thus

$$\begin{aligned} \prod_{t' \neq t} p(b_{t'}) &= \underbrace{\left(\prod_{t' \neq t} A_{t'}\right)}_{\mathcal{A}_t} \cdot \exp\left(\sum_{t' \neq t} \frac{b_{t'} \lambda_{\mathrm{PRIOR}}(b_{t'})}{2}\right) \\ &= \mathcal{A}_t \exp\left(\frac{\boldsymbol{b}_t^{\mathrm{T}} \boldsymbol{\lambda}_{\mathrm{PRIOR},t}}{2}\right) \end{aligned}$$

where $\boldsymbol{b}_t$ contains $\hat{\boldsymbol{b}}$ except b_t and $\boldsymbol{\lambda}_{\mathrm{PRIOR},t}$ contains the *a priori* probabilities of the elements of $\boldsymbol{b}_t$. Finally, after simplification, we obtain

$$\lambda_{\mathrm{EXT}}(b_t) = \ln\left(\frac{\sum_{\hat{\boldsymbol{b}} \in \mathbb{B}_t^+} p(\hat{\boldsymbol{z}}|\hat{\boldsymbol{b}}) \cdot \exp\left(\frac{\boldsymbol{b}_t^{\mathrm{T}} \boldsymbol{\lambda}_{\mathrm{PRIOR},t}}{2}\right)}{\sum_{\hat{\boldsymbol{b}} \in \mathbb{B}_t^-} p(\hat{\boldsymbol{z}}|\hat{\boldsymbol{b}}) \cdot \exp\left(\frac{\boldsymbol{b}_t^{\mathrm{T}} \boldsymbol{\lambda}_{\mathrm{PRIOR},t}}{2}\right)}\right).$$

Knowing $\boldsymbol{b}_t^{\mathrm{T}} \boldsymbol{\lambda}_{\mathrm{PRIOR},t} = \hat{\boldsymbol{b}}^{\mathrm{T}} \boldsymbol{\lambda}_{\mathrm{PRIOR}} - b_t \lambda_{\mathrm{PRIOR}}(b_t)$ and $p(\hat{\boldsymbol{z}}|\hat{\boldsymbol{b}}) \propto \exp\left(-\frac{1}{\sigma^2}\|\hat{\boldsymbol{z}} - \hat{\boldsymbol{R}}_\Gamma \hat{\boldsymbol{F}} \hat{\boldsymbol{b}}\|^2\right)$, and using the max-log approximation [7] the extrinsic probability becomes

$$\begin{aligned} \lambda_{\mathrm{EXT}}(b_t) \approx \quad & \max_{\hat{\boldsymbol{b}} \in \mathbb{B}_t^+} \left(-\tfrac{1}{\sigma^2}\|\hat{\boldsymbol{z}} - \hat{\boldsymbol{R}}_\Gamma \hat{\boldsymbol{F}} \hat{\boldsymbol{b}}\|^2 + \frac{\hat{\boldsymbol{b}}^{\mathrm{T}} \boldsymbol{\lambda}_{\mathrm{PRIOR}}}{2}\right) \\ & - \max_{\hat{\boldsymbol{b}} \in \mathbb{B}_t^-} \left(-\tfrac{1}{\sigma^2}\|\hat{\boldsymbol{z}} - \hat{\boldsymbol{R}}_\Gamma \hat{\boldsymbol{F}} \hat{\boldsymbol{b}}\|^2 + \frac{\hat{\boldsymbol{b}}^{\mathrm{T}} \boldsymbol{\lambda}_{\mathrm{PRIOR}}}{2}\right) \\ & - \lambda_{\mathrm{PRIOR}}(b_t). \end{aligned}$$

To maximize the two expressions above, it is useful to find a vector $\boldsymbol{\Lambda}$ satisfying $4(\hat{\boldsymbol{R}}_\Gamma \hat{\boldsymbol{F}})^{\mathrm{T}} \boldsymbol{\Lambda} = \sigma^2 \boldsymbol{\lambda}_{\mathrm{PRIOR}}$. This allows writing

$$\begin{aligned} & \max\left\{-\tfrac{1}{\sigma^2}\|\hat{\boldsymbol{z}} - \hat{\boldsymbol{R}}_\Gamma \hat{\boldsymbol{F}} \hat{\boldsymbol{b}}\|^2 + \frac{\hat{\boldsymbol{b}}^{\mathrm{T}} \boldsymbol{\lambda}_{\mathrm{PRIOR}}}{2}\right\} \\ & \qquad = \max\left\{-\tfrac{1}{\sigma^2}\|\hat{\boldsymbol{z}} - \hat{\boldsymbol{R}}_\Gamma \hat{\boldsymbol{F}} \hat{\boldsymbol{b}}\|^2 + 2\frac{\left(\hat{\boldsymbol{R}}_\Gamma \hat{\boldsymbol{F}} \hat{\boldsymbol{b}}\right)^{\mathrm{T}} \boldsymbol{\Lambda}}{\sigma^2}\right\} \\ & \qquad = -\tfrac{1}{\sigma^2} \min \|\hat{\boldsymbol{z}} + \boldsymbol{\Lambda} - \hat{\boldsymbol{R}}_\Gamma \hat{\boldsymbol{F}} \hat{\boldsymbol{b}}\|^2 + \mathrm{c}, \end{aligned}$$

where c is not dependent on $\hat{\boldsymbol{b}}$. For instance, it can be easily checked that the vector $\boldsymbol{\Lambda}$ defined as $\boldsymbol{\Lambda} = \frac{\sigma^2}{2u_{D-1}}[0, \ldots, 0, \lambda_{\mathrm{PRIOR}}(1), \ldots, 0, \ldots, 0, \lambda_{\mathrm{PRIOR}}(T)]^{\mathrm{T}} \in \mathbb{R}^{2TD}$ is a valid solution.

Let us now define $\boldsymbol{b}_{\mathrm{SD}}$ the ML solution of the equation $\operatorname{argmin} \|\hat{\boldsymbol{z}} + \boldsymbol{\Lambda} - \hat{\boldsymbol{R}}_\Gamma \hat{\boldsymbol{F}} \hat{\boldsymbol{b}}\|^2$, and s the sign of its $t-$th element $b_{\mathrm{SD}}(t)$. The *extrinsic* probability is simplified to

$$\begin{aligned} \lambda_{\mathrm{EXT}}(b_t) = \quad & -\frac{b_{\mathrm{SD}}(t)}{\sigma^2}\|\hat{\boldsymbol{z}} + \boldsymbol{\Lambda} - \hat{\boldsymbol{R}}_\Gamma \hat{\boldsymbol{F}} \boldsymbol{b}_{\mathrm{SD}}\|^2 \\ & + \frac{b_{\mathrm{SD}}(t)}{\sigma^2} \min_{\boldsymbol{b} \in \mathbb{B}_t^{-s}} \|\hat{\boldsymbol{z}} + \boldsymbol{\Lambda} - \hat{\boldsymbol{R}}_\Gamma \hat{\boldsymbol{F}} \boldsymbol{b}\|^2 \\ & - \lambda_{\mathrm{PRIOR}}(b_t), . \end{aligned}$$

Denoting $\boldsymbol{b}_{\mathrm{SD},t}$ the solution of $\underset{\boldsymbol{b} \in \mathbb{B}_t^{-s}}{\operatorname{argmin}} \|\hat{\boldsymbol{z}} + \boldsymbol{\Lambda} - \hat{\boldsymbol{R}}_\Gamma \hat{\boldsymbol{F}} \boldsymbol{b}\|^2$, we obtain

$$\begin{aligned} \lambda_{\mathrm{EXT}}(b_t) = \quad & -\frac{b_{\mathrm{SD}}(t)}{\sigma^2}\|\hat{\boldsymbol{z}} + \boldsymbol{\Lambda} - \hat{\boldsymbol{R}}_\Gamma \hat{\boldsymbol{F}} \boldsymbol{b}_{\mathrm{SD}}\|^2 \\ & + \frac{b_{\mathrm{SD}}(t)}{\sigma^2}\|\hat{\boldsymbol{z}} + \boldsymbol{\Lambda} - \hat{\boldsymbol{R}}_\Gamma \hat{\boldsymbol{F}} \boldsymbol{b}_{\mathrm{SD},t}\|^2 \\ & - \lambda_{\mathrm{PRIOR}}(b_t), . \end{aligned} \qquad (7)$$

The $4T+1$ vectors $\boldsymbol{b}_{\mathrm{SD}}$ and $\boldsymbol{b}_{\mathrm{SD},t}$ can be computed using hard sphere decoding, $\boldsymbol{\lambda}_{\mathrm{PRIOR}}$ is given by the soft inputs from the iterative receiver.

3.4 Iterative Receiver with Subspace-based Sphere Decoder

We use the subspace-based implementation of the sphere decoder that has been presented and detailed in [1]. To summarize, this implementation making use of the subspace structure and the channel model presented in Sec. 2 allows saving complexity by performing only one QR-decomposition

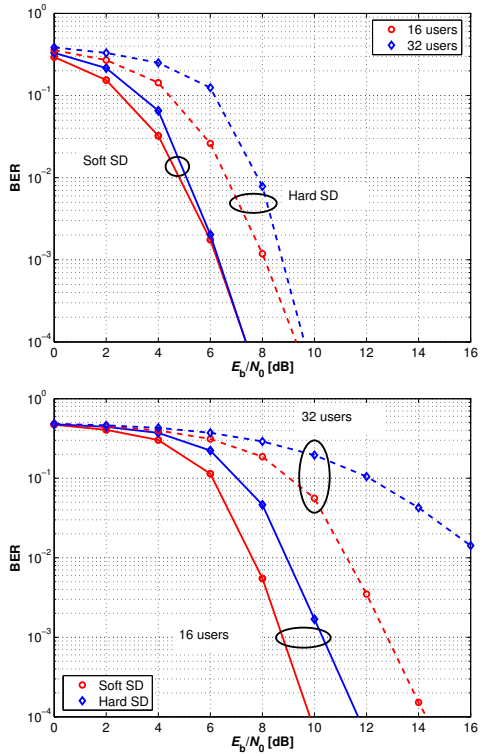

Figure 2: **Hard vs Soft Sphere Decoder:** BER versus SNR after 4 receiver iteration for $K \in \{16, 32\}$ users. The channel is perfectly known (top) or estimated (bottom).

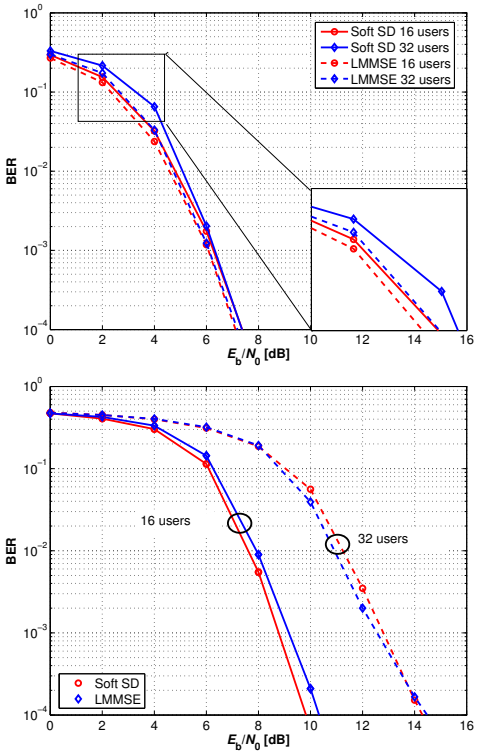

Figure 3: **Soft Sphere Decoder vs LMMSE** BER versus SNR after 4 receiver iterations for $K \in \{16, 32\}$ users. The channel is perfectly known (top) or estimated (bottom) at the receiver.

valid for a whole data block (see (5)) instead of one per data symbol. This implies modifications of the sphere decoder algorithm into a block structured sphere decoder. The details can be found in [1]. Note that the algorithm in [1] performs hard-sphere decoding and is used to compute the $4T + 1$ vectors $\boldsymbol{b}_{\mathrm{SD}}$ and $\boldsymbol{b}_{\mathrm{SD},t} \in \{1, \ldots, 2T\}$ needed for the log-likelihood ratios in (7).

The soft outputs of the sphere decoder $\boldsymbol{\lambda}_{\mathrm{PRIOR}}$ are sent to a BCJR decoder [6], which provides *extrinsic* and *a posteriori* probabilities on the data bits. Both are fed back for the next receiver iteration (see Figure 1). The *a posteriori* probabilities are used for channel estimation (see [3]). The *a priori* probabilities needed as soft input for the sphere decoder are computed using $\boldsymbol{\lambda}_{\mathrm{PRIOR}} = \boldsymbol{\lambda}_{\mathrm{POST}} - \boldsymbol{\lambda}_{\mathrm{EXT}}$, see (6)

4. SIMULATION RESULTS

The realizations of the time-varying frequency-selective channel are generated using an exponentially decaying power delay profile with root mean square delay spread $T_{\mathrm{D}} = 4T_{\mathrm{C}} = 1\mu$s for a chip rate of $1/T_{\mathrm{C}} = 3.84 \cdot 10^6\,\mathrm{s}^{-1}$ [8]. We assume $L = 15$ resolvable paths. The autocorrelation for every channel tap is given by the classical Clarke spectrum [9]. The system operates at carrier frequency $f_C = 2\,$GHz and the users move with velocity $v = 70\mathrm{kmh}^{-1}$. These gives a Doppler bandwidth of $B_{\mathrm{D}} = 126$Hz. We use $T = R = 4$ transmit and receive antennas and $N = 64$ subcarriers. A data block consists of $M = 256$ OFDM symbols including $J = 60$ pilot symbols. The system is designed for $v_{\max} = 102.5\,\mathrm{kmh}^{-1}$ which results in a dimension $D = 3$ for the Slepian basis expansion. The MIMO channel taps are normalized in order to analyze the diversity gain of the receiver only. No antenna gain is present due to this normalization.

For data transmission, a convolutional, non-systematic, non-recursive, 4 state, rate $R_C = 1/2$ code with code generators $(5, 7)_8$, is used. All illustrated results are obtained by averaging over 100 independent channel realizations. We define the signal-to-noise ratio $E_b/N_0 = PM/\left(2R_C\sigma^2 N(M-J)\right)$, taking into account the loss due to coding, pilots and cyclic prefix. The noise variance σ^2 is assumed to be known at the receiver.

The following simulations have been performed:

• **Hard Sphere Decoder vs Soft Sphere Decoder** A comparison of the performance of soft and hard sphere decoders is shown in Fig. 2. Using soft input soft output sphere decoder allows at least 2dB gain over hard sphere decoding.

• **Soft Sphere Decoder vs LMMSE** We compare the performance of the soft sphere decoder on a per user basis to the performance of a LMMSE equalizer detecting jointly all users in Fig. 3. Both detection methods perform similar.

5. ON THE COMPUTATIONAL COMPLEXITY

We define a *flop* as a floating point operation (addition, substraction, multiplication, division or square root) in the *real* domain [10]. Thus, one complex multiplication (CM) requires 4 real multiplications and 2 additions, leading to 6 *flops*. Similarly, one complex addition (CA) requires 2 *flops*. We denote by $q_t \leq Q^{(T-t+1)}$ the number of candidates after the step t of the sphere decoder (see [1] for details). q_t is a random variable since it depends on the realization of $\boldsymbol{b}$, $\hat{\boldsymbol{S}}$ and $\boldsymbol{n}$. $Q = |\mathcal{A}|$ is the size of the alphabet.

5.1 Hard Sphere Decoder

As given in [1], the computational complexity for a block of length $M - J$ using hard sphere decoding requires:

- one *thin* complex QR factorization of size $NR \times DT$, with

computational complexity [10]

$$c_{\mathrm{QR}} = 8(DT)^2 \left(NR - \frac{DT}{3} \right) \, flops \, ,$$

- $M - J$ runs of the hard sphere decoder with complexity

$$\begin{aligned} c_{\mathrm{hard}}[m] = \quad & 2D \sum_{t=1}^{T-1} \left[(T-t)(4D+3) - 2D + 1 \right] q_{t+1}[m] \\ & + 4(T-1)DQ(D+2) \, flops \, . \end{aligned}$$

An upper bound of this expression can be computed using $q_t = Q^{(T-t+1)}$, which corresponds to the case where all combinations remain valid candidate at all steps. This is equivalent to an exhaustive search using the sphere decoder implementation and an infinite radius:

$$\begin{aligned} c_{\mathrm{hard}}[m] \leq \quad & 2D(4D+3) \sum_{t=1}^{T-1} tQ^t - 2D(2D-1) \sum_{t=1}^{T-1} Q^t \\ & + 4(T-1)DQ(D+2) \, flops \, . \end{aligned} \tag{8}$$

The computational complexity for a single data block can be upper bounded using (8) and $C_{\mathrm{hard}} = c_{\mathrm{QR}} + \sum_{m \notin \mathcal{P}} c_{\mathrm{hard}}[m]$.

5.2 Soft Sphere Decoder

Computations are very similar except that they are done in the real domain. Thus dimension are multiplied by a factor 2. However, we have now real multiplications and additions, equivalent to one *flop* each. Furthermore, the alphabet size is reduced to $Q/2$. The computations required are:

- one *thin* real QR factorization of size $2NR \times 2DT$, with computational complexity [10]

$$c_{\mathrm{QR}} = 8(DT)^2 \left(NR - \frac{2DT}{3} \right) \, flops \, ,$$

- $(M-J)(4T+1)$ runs of the subspace based sphere decoder with complexity

$$\begin{aligned} c_{\mathrm{soft}}[m] = \quad & D \sum_{t=1}^{2T-1} \left[(2T-t)(2D+1) - D \right] q_{t+1}[m] \\ & + (2T-1)DQ(D+1)/2 \, flops \, . \end{aligned}$$

As previously, an upper bound of this expression can be computed using $q_t = \left(\frac{Q}{2}\right)^{(2T-t+1)}$:

$$\begin{aligned} c_{\mathrm{soft}}[m] \leq \quad & D(2D+1) \sum_{t=1}^{2T-1} t \left(\tfrac{Q}{2}\right)^t - D \sum_{t=1}^{2T-1} \left(\tfrac{Q}{2}\right)^t \\ & + (2T-1)DQ(D+1)/2 \, flops \, . \end{aligned} \tag{9}$$

The complexity for a single data block can be upper bounded using (9) and $C_{\mathrm{soft}} = c_{\mathrm{QR}} + (4T+1) \sum_{m \notin \mathcal{P}} c_{\mathrm{soft}}[m] \, .$

5.3 Comparison of the computational complexity

In Fig. 4 we show upper bounds of the iterative receiver complexity over a block of size $M - J$ using, respectively, hard sphere decoder, soft sphere decoder and linear minimum mean square error (LMMSE), see for example [11] for details. We can see that the soft sphere decoder is about one order of magnitude more complex than the hard sphere decoder and one order of magnitude less complex than LMMSE detection.

6. CONCLUSIONS

We have presented a subspace based implementation of a soft sphere decoder, making use of the basis expansion channel model.

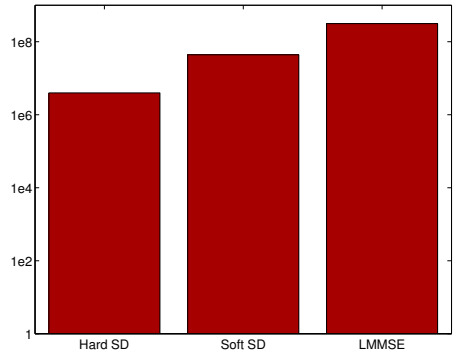

Figure 4: **Upper bound for the complexity per user:** we show the maximum computational complexity using hard sphere decoding as in [1], soft sphere decoding or LMMSE.

This allows for complexity reduction when the channels are time-varying. The use of soft outputs is a compromise between complexity and performance. The soft sphere decoder performs close to the LMMSE filter, while saving one order of magnitude of complexity.

REFERENCES

[1] C. Dumard and T. Zemen, "Subspace based sphere decoder for MC-CDMA in time-varying MIMO channels," in *Proc. 18th IEEE PIMRC*, Athens, Greece, September 2007.

[2] R. Wang and G. B. Giannakis, "Approaching MIMO channel capacity with reduced-complexity soft sphere decoding," in *Proc. Wireless Communications and Networking Conference (WCNC)*, Atlanta, Georgia, USA, March 2004.

[3] T. Zemen and C. F. Mecklenbräuker, "Time-variant channel estimation using discrete prolate spheroidal sequences," *IEEE Trans. Signal Processing*, vol. 53, no. 9, pp. 3597–3607, September 2005.

[4] D. Slepian, "Prolate spheroidal wave functions, Fourier analysis, and uncertainty - V: The discrete case," *The Bell System Technical Journal*, vol. 57, no. 5, pp. 1371–1430, May-June 1978.

[5] J. Wehinger, "Iterative multi-user receivers for CDMA systems," Ph.D. dissertation, Vienna University of Technology, Vienna, Austria, July 2005.

[6] L. R. Bahl, J. Cocke, F. Jelinek, and J. Raviv, "Optimal decoding of linear codes for minimizing symbol error rate," *IEEE Trans. Inform. Theory*, vol. 20, no. 2, pp. 284–287, Mar. 1974.

[7] B. M. Hochwald and S. ten Brink, "Achieving near-capacity on a multiple-antenna channel," *IEEE Trans. Commun.*, vol. 51, no. 3, pp. 389–399, march 2003.

[8] L. M. Correia, *Wireless Flexible Personalised Communications*. Wiley, 2001.

[9] R. H. Clarke, "A statistical theory of mobile-radio reception," *The Bell System Technical Journal*, vol. 47, pp. 957–1000, July/August 1968.

[10] G. H. Golub and C. F. V. Loan, *Matrix Computations*, 3rd ed. Baltimore (MD), USA: Johns Hopkins University Press, 1996.

[11] C. Dumard and T. Zemen, "Low-complexity MIMO multiuser receiver: A joint antenna detecion scheme for time-varying channels," *IEEE Trans. Signal Processing*, 2008, in print.